

# Influence of liquid flow conditions on spray characteristics of internal-mixing twin-fluid atomizers

A. Kufferath<sup>\*</sup>, B. Wende, W. Leuckel

Engler-Bunte-Institut, Bereich Feuerungstechnik, Universität Karlsruhe (TH), D-76128 Karlsruhe, Germany

## Abstract

For an internal-mixing twin-fluid atomizer with coaxial liquid feed the dependence of the spray characteristics on the liquid flow conditions, i.e. laminar, turbulent or cavitating, has been investigated. Results obtained with Phase Doppler Analyzer, high speed photography and pressure drop measurements were correlated with the nozzle geometry and the flow rates of liquid and gas. The investigated nozzle allowed variation of five geometric parameters, the most important ones being the liquid inlet port diameter, the nozzle outlet port diameter and the length of the outlet port. The volume flow rate of the liquid  $\dot{V}_L$  ranged from 5 to 100 L/h, and of the compressed air  $\dot{V}_A$  from 1 to 20 m<sup>3</sup>/h. For visualizing the internal flow, an optically accessible planar nozzle of comparable geometry has been used. It was observed that flow conditions of the liquid jet leaving the inlet port have a strong influence on the distributions of the  $D_{32}$  droplet diameter along radial traverses across the spray. For short outlet ports ( $l_o/d_o \lesssim 2$ ), the maximal  $D_{32}$  for laminar liquid jet is always found on the spray axis, whereas a turbulent liquid jet leads to nearly even profiles. For long outlet ports ( $l_o/d_o \gtrsim 4$ ) even profiles are found in either case. © 1999 Elsevier Science Inc. All rights reserved.

**Keywords:** Twin-fluid atomization; Primary breakup; Breakup modes; Laminar–turbulent transition; Flow visualization

## Notation

ALR	air-to-liquid mass ratio (–)
$d$	inlet/outlet port diameter (mm)
$D_{32}$	Sauter Mean Diameter ( $\mu\text{m}$ )
$l$	inlet/outlet port length (mm)
$\dot{m}$	liquid mass flux density ( $\text{kg}/(\text{m}^2\text{s})$ )
$p$	pressure beyond atmospheric (bar)
$r$	radius (mm)
$u$	axial velocity (m/s)
$\dot{V}$	volume flow rate (L/h, m <sup>3</sup> /h)
$z$	distance downstream of the nozzle (mm)
$Re$	liquid flow Reynolds number $Re = u_L d_i \rho_L / \eta_L$ (–)
$\eta$	dynamic viscosity (Pa s)
$\rho$	density ( $\text{kg}/\text{m}^3$ )
$\sigma$	surface tension (N/m)

## Subscripts

A	air (–)
i	inlet port for the liquid (–)
L	liquid (–)
mean	mean (–)
n	standard temperature and pressure (–)
o	outlet port of the nozzle (–)

## 1. Introduction

In many industrial applications such as spray-drying, exhaust cleaning and combustion, well defined spray characteristics and a wide flow rate operation range are required. In most cases air-assisted atomizers are able to fulfil these requirements and are used, therefore, despite their additional energy consumption. As a group, air-assisted atomizers can be divided into internal and external mixing types, depending on where the first contact between the liquid and gas phase takes place. If abrasion and fouling are unimportant, internal-mixing atomizers are preferred due to their more efficient energy transfer from gas to liquid. From this category, the Y-jet atomizer, the mixing chamber atomizer, the effervescent atomizer, and the internal-mixing atomizer with coaxial liquid feed are the most common ones in chemical engineering and combustion applications. The last of these will be the subject of this paper.

In the past, the performance of air-assisted internal-mixing atomizers with coaxial liquid feed has been investigated in order to clarify the effects of nozzle design, load, liquid and gas properties on spray characteristics (Nukiyama and Tanasawa, 1938–1939 Lorenzetto and Lefebvre, 1977). Results of these investigations are semi-empirical equations which yield a characteristic droplet diameter as a function of those parameters. In the corresponding relationships, the governing property is the velocity slip between the liquid jet and the surrounding gas. Quite often a second term is added to account for the dependence on the liquid viscosity, which leads to an increase of the resulting droplet diameter for liquids of

<sup>\*</sup> Corresponding author. E-mail: andreas.kufferath@ciw.uni-karlsruhe.de

higher viscosity. These equations are of a similar type as the attempts to correlate a diameter with the Weber and Ohnesorge number. They are only applicable for any particular atomizer within the investigated ranges. Extrapolations seem impossible, since the physical basis of the equations is weak as the disintegration process is not yet fully understood (Chigier, 1991). The process consists of many successive and simultaneous steps, i.e. the rearrangement of the liquid velocity profile after exiting from the liquid insert (Schweitzer, 1937), the generation of small scale disturbances on the liquid surface, the onset of breakup (Wu and Faeth, 1993), the disintegration of the jet (Faragó and Chigier, 1992), and finally the breakup of ligaments and droplets (Gelfand, 1996). Detailed knowledge of these single steps provides the possibility of interpreting a more complex disintegration process of the liquid.

For the internal-mixing twin-fluid atomizer with coaxial liquid feed, the influence of liquid flow conditions on spray characteristics has not yet been the subject of detailed published research. Investigations focussed mainly on the influence of the relative velocity between the liquid jet and the surrounding air. As a result, the liquid is usually injected with low velocity in order to maximize the relative velocity between the liquid flow and the atomizing air. The important influence of liquid turbulence for an improved and accelerated breakup of the liquid jet has even been doubted (Lefebvre, 1989). In contrast to this assumption, Sato et al. 1988 presented results of a similar atomizer type for the atomization of coal–water mixtures. In this case an efficient atomization has been achieved by increasing the interfacial perturbation between liquid and air in the exit port of the atomizer and promoting the turbulence of the liquid supplied to the atomizer.

On the other hand it is also well known from investigations dealing with injecting a liquid jet into quiescent air, that the turbulence of the liquid jet has an important influence on jet breakup. It must be noted for those experiments that the relative velocity between air and liquid is only inverted but should have the same effect, namely to propagate an initial disturbance amplitude (Mansour and Chigier, 1994). In combination with the dynamic pressure of the air any initial disturbance starts an enhanced breakup. Concerning this aspect, the importance of the turbulent boundary layer for the breakup of the liquid jet was investigated by Wu et al., 1995. They stripped off the turbulent boundary layer of a not fully developed turbulent liquid flow with a cutter mechanism. With this removal of the boundary layer it was possible to generate liquid jets with a Reynolds number greater than  $10^5$  with a smooth surface. The influence of air flow turbulence on the breakup mechanism is virtually unexplained, though recently this influence became a subject of research (Shavit and Chigier, 1994). Investigations concerning the influence of cavitation on jet breakup were undertaken by many research facilities, but for the atomizing system presented here cavitation is of minor importance. Summarizing, one may assume that, for the investigated internal-mixing twin-fluid with coaxial liquid feed, the effect of liquid flow conditions on the break up process cannot be neglected.

As mentioned above, the spray characteristics of an internal-mixing air-assisted atomizer strongly depend on the interaction of gas and liquid inside the nozzle, where the difference in velocity of the two phases is sufficiently high to disintegrate the liquid jet. In this zone, the major part of ligament formation and further droplet breakup takes place. This study focusses on the influence of liquid flow conditions upon the atomization process and the resulting spray characteristics. The flow condition of the liquid when entering the mixing chamber is determined by the volumetric flow rate, the viscosity, and the geometry of the inlet port. The two main liquid flow regimes, laminar and turbulent, result in different struc-

tures of the liquid jet surface leaving the duct of the liquid insert. In the laminar case the surface is smooth whereas, for the turbulent liquid jet, distortions on the surface are present. They provide the target for aerodynamic shear forces and, therefore, will lead to improved disintegration. In addition, the occurrence of cavitation can lead to a drastic change of the flow pattern of the liquid jet. Both, transition from laminar to turbulent and onset of cavitation, may lead to a major change in spray characteristics.

## 2. Experimental

The design of the nozzle used for most of the parametric studies described in this paper is shown in Fig. 1. The pressurized air is fed through the annular slot (b), and the liquid is fed through the inlet port (a). After the first contact of air and liquid, a two-phase flow develops in the outlet port (c). Due to the flexible construction, the length  $l_o$  ( $0 \leq l_o \leq 16$  mm) and the diameter  $d_o$  ( $1.1 \leq d_o \leq 4.8$ ) of the outlet port and the length  $l_i$  and the diameter  $d_i$  ( $0.4 \leq d_i \leq 2.0$  mm) of the inlet port can be varied independently. The length to diameter ratio  $l_i/d_i$  for the inlet port varied between 5 and 20. For the visualization of the processes which take place inside the nozzle a planar, optically accessible nozzle with a square cross section ( $3 \times 3$  mm) outlet port has been used. For optical access, two sides of this planar nozzle were made out of acrylic glass. Details of the design and the geometric parameters of this nozzle were published in Kufferath and Leuckel (1997). The transferability of the results obtained with the optically accessible planar nozzle for the rotationally symmetric nozzle was checked out beforehand.

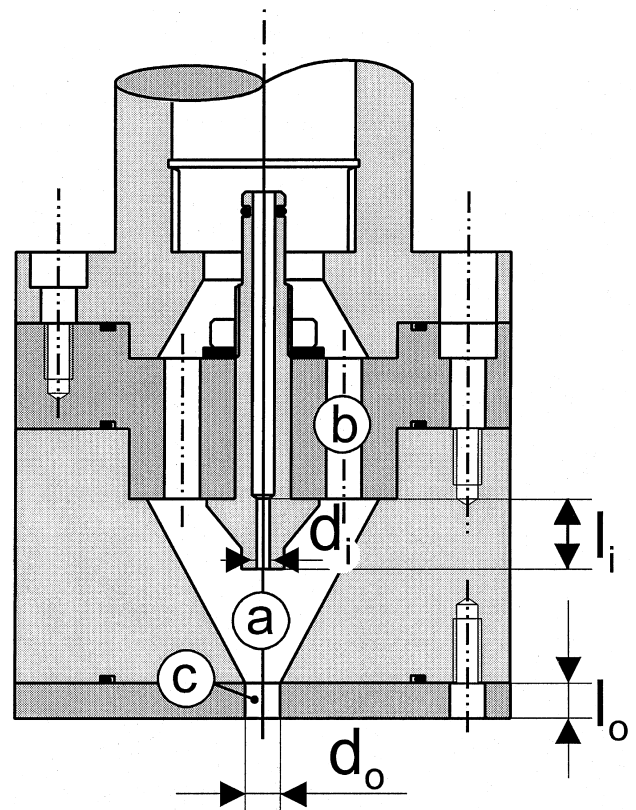


Fig. 1. Investigated internal mixing nozzle system.

Most experiments were conducted using a glycol–water mixture at 25°C as a test liquid ( $\rho = 1084 \text{ kg/m}^3$ ,  $\eta = 5 \times 10^{-3} \text{ Pas}$ ,  $\sigma = 48 \times 10^{-3} \text{ N/m}$ ). The spray is locally characterized by droplet diameter, droplet velocity and volume flux density. This information is obtained by spatially resolving phase doppler analyzer (PDA) measurements 200 mm downstream of the nozzle exit where no further droplet breakup occurs and the spray density allows reliable PDA measurements over a wide range of flow rates. Photos of the flow structures and the break up process in-and outside the nozzle were taken using a nanolite spark in combination with a synchronized reflex camera. The spark has a duration time of approximately 20 ns which is sufficiently short to freeze the motion of the liquid phase. Due to the difficulties in determining accurately the local mass flux density with the PDA, an isokinetic sampling of the liquid fraction was used. The accuracy of the balance when integrating the local mass flux densities over the entire cross section was better than 90%, even in the nozzle near field at a distance 25 mm downstream of the nozzle. A detailed description of the complete test rig is published elsewhere (Kufferath et al., 1996).

### 3. Results and discussion

First, examples of the qualitative influence of liquid flow conditions on spray characteristics are shown. In the phe-

nomenological description the main liquid flow regimes: laminar, turbulent and cavitating, are illustrated. In the second part, the separate variation of the governing parameters for the laminar–turbulent transition of the liquid flow is being investigated. The onset of cavitation and its effect on spray characteristics is the subject of the third part. Finally, other influences apart from liquid flow conditions, such as the gas flow rate, the geometry of the outlet port and the length of the mixing chamber, on transition between the different flow regimes of the liquid phase and on the resulting spray characteristics are presented.

#### 3.1. Phenomenological description

In Fig. 2, upper part, the pressure drop on the air side is plotted against the liquid volume flow rate or the liquid Reynolds number ( $Re_L$ ), respectively. The values are specific for constant gas flow rate and fixed nozzle geometry. High speed photos of the disintegration process inside and outside the optically accessible nozzle – corresponding to the four most important regimes – are assigned to the diagram.

For very low liquid volume flow rate (I), disintegration of the liquid jet, is completed before reaching the outlet port. The bulk of the liquid impacts on the inner wall surface of the nozzle and approaches the outlet as a wall film. Therefore, satisfactory atomization cannot be achieved. With increasing liquid volume flow rate (II) stationary atomization starts. In

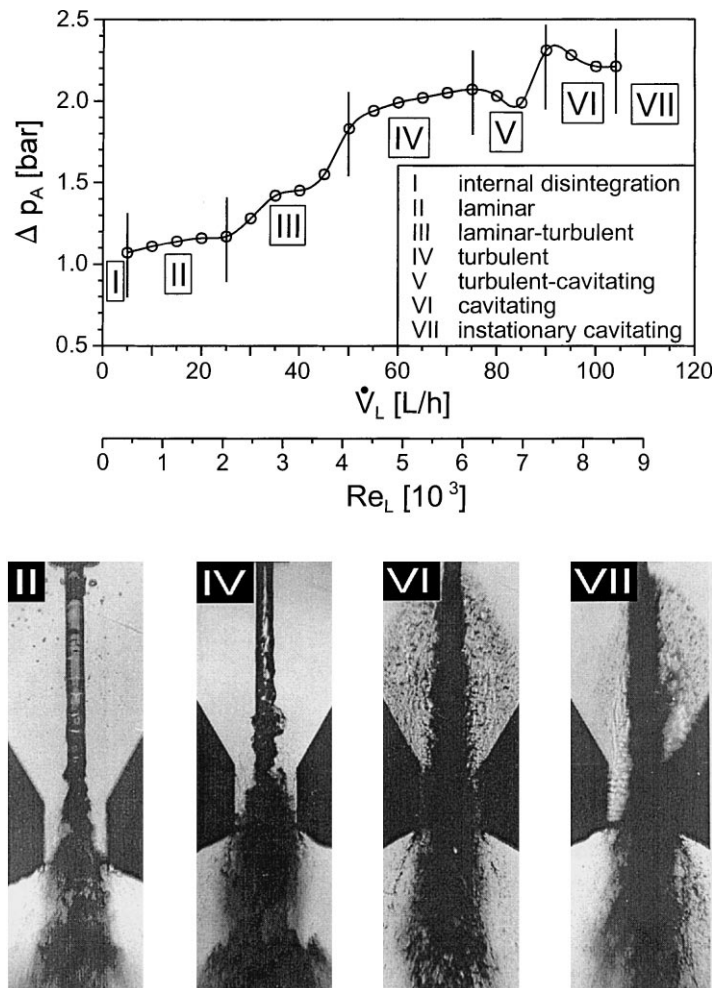


Fig. 2. Air pressure drop  $\Delta p_A$  as a function of liquid volume flow rate  $\dot{V}_L$  and flow characteristics inside the nozzle.

this regime the pressure drop weakly depends on the liquid volume flow rate. Disintegration of the laminar liquid jet starts just above the outlet port where the differences in velocity between the slowly flowing liquid jet and the fast flowing air are high enough to generate the first visible disturbances on the surface. At the end of the outlet port, marked by the horizontal lower edge of the acrylic glass window, the cross-section is not homogeneously filled with two-phase flow. Therefore, part of the air passes the nozzle as an annular coflow without really contributing to the atomization process. Further increase of the liquid volume flow rate (III) causes a strong increase of pressure drop. This regime is characterized by sudden changes of spray characteristics and pressure drop, the atomization process becomes non-stationary, accompanied by the emission of high-pitch sound. The frequency of pressure fluctuations and changes in spray characteristics is about 1 Hz. When applying the PDA for the measurement of time resolved measurements of droplet arrival statistics in this transition region ( $Re = 3250$ ), these sudden changes in pressure drop could well be correlated with the changes in spray characteristics. At the spray axis the laminar state is characterized by an increase in the frequency of the occurrence of bigger droplets. As a stationary atomization process cannot be achieved there, this transition between the laminar (II) and the turbulent (IV) flow regime of the liquid excludes technical applications. As in the laminar case, for the turbulent liquid flow (IV) the pressure drop again increases slowly with the liquid volume flow rate. The atomization process is now steady again. Disintegration starts shortly after the inlet port. The cross-section at the end of the outlet port is nearly completely filled with two-phase flow. Therefore, better energy transfer from the gas to the liquid than in the laminar case is being obtained. For still higher liquid volume flow rate, an unsteady transition (V) to cavitation (VI) takes place, accompanied by another increase of pressure drop. It must be noted, however, that this transition is not correlated with Reynolds number and, consequently, does not necessarily start in the turbulent region. The disintegration process in the cavitation regime is similar to the turbulent case. The improvement of the disintegration process and droplet formation is not remarkable. For higher volume flow rate (VII) cavitation becomes unstable. The liquid jet is deflected off the nozzle axis. The pressure drop may decrease drastically because the cross-section of the outlet port is now partly released. A great deal of air leaves the outlet port without contributing to the atomization process. As a result, the atomization quality deteriorates and a strong imbalance of the droplet diameter distribution and the mass flux density over the cross-section can be observed. For very high liquid flow rates and moderate air pressures in the mixing chamber also a hydraulic flip (Yule et al., 1998) of the liquid jet was observed. In the absence of distortions of a sufficiently high amplitude, the liquid jet after the hydraulic flip showed a delayed primary breakup, resulting in very poor atomization.

When investigating a liquid jet in quiescent air, the regions of transition from laminar to turbulent are comparable. It can be concluded, therefore, that transition (III) between two atomization regimes is caused by liquid flow properties which are correlated with the liquid Reynolds number. On the other hand, the onset of cavitation strongly depends on the pressure inside the mixing chamber, liquid inlet geometry (Ramamurthi and Nandakumar, 1994) and manufacturing imperfections (Ohrn et al., 1991) and, hence, cannot be described by liquid flow properties alone.

### 3.2. Governing parameters for the laminar–turbulent transition

Since transition can be correlated with the liquid Reynolds number, it depends on the liquid volume flow rate, the diam-

eter of the inlet port, and the liquid viscosity. The inlet port diameter  $d_i$  has been varied between 0.6 and 1.95 mm (denoted as 1.9 mm) for constant gas flow rates, outlet port lengths and diameters. Fig. 3 shows the pressure drop of the air as a function of the Reynolds number for four inlet port diameters ( $l_i/d_i = 10$ ). There is a sudden increase in the pressure drop for  $Re \geq 3000$ , except for the smallest diameter investigated. In this case a gradual pressure increase could be observed. For  $d_i = 0.9$  and 1.3 mm a transition region from  $Re \approx 2000$  to  $Re \approx 3000$  occurs, whereas for  $d_i = 0.6$  mm no transition region could be found. These differences in the appearance of transition can be explained by the formation of disturbances. The smaller the diameter, the more important are external influences such as manufacturing imperfections. For the smallest diameter it was even impossible to generate a jet with laminar appearance. This jet is transparent, but has a large scale helix structure. Therefore, these smallest inlet ports could not be investigated in detail.

As mentioned before, transition between laminar and turbulent liquid flow is related to a drastic change of spray characteristics. Fig. 4 shows spatial  $D_{32}$  distributions for two

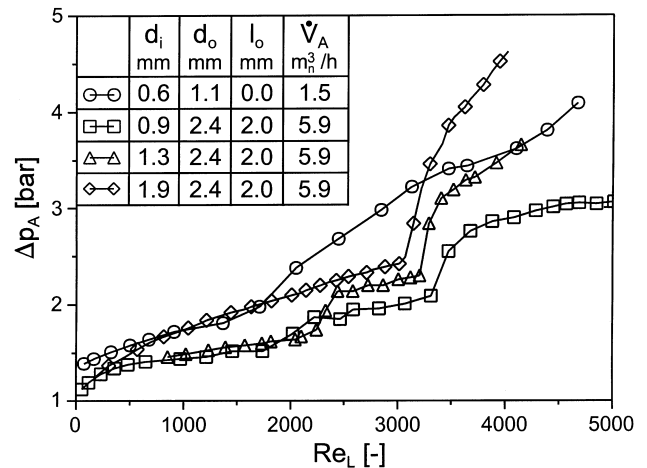


Fig. 3. Air pressure drop  $\Delta p_A$  as a function of liquid flow Reynolds number and inlet port diameter  $d_i$ .

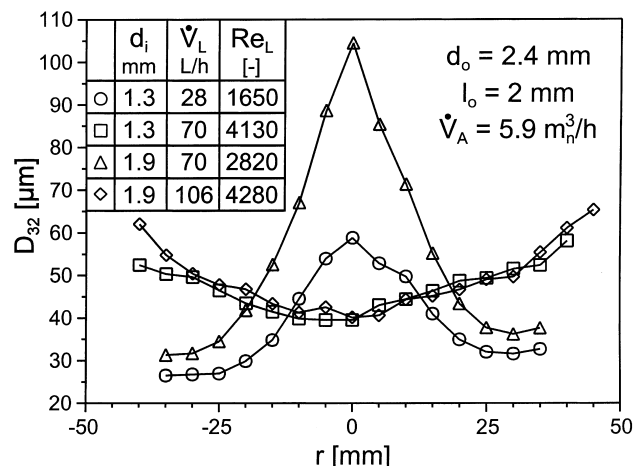


Fig. 4. Radial profiles of local  $D_{32}$  as a function of inlet port diameter  $d_i$  and liquid volume flow rate  $\dot{V}_L$ .

inlet port diameters, related to both flow regimes ( $l_i/d_i = 10$ ). In both laminar cases the maximum of the  $D_{32}$  could be observed at the spray axis. At the spray boundary the  $D_{32}$  mean droplet diameter is far smaller. As in Fig. 2-II, air leaving the nozzle with high velocity led to disintegration of the liquid into fine droplets just in the outer zones of the spray. A complete disintegration of the ligaments near the spray axis could not be achieved, however. In contrast to the laminar case, no ligaments can be seen at the bottom of the photograph for the turbulent case (Fig. 2-IV). At the nozzle exit, liquid phase disintegration is nearly complete. This corresponds to the result that in both turbulent cases a nearly even profile of the  $D_{32}$  was obtainable.

According to Fig. 5, for constant liquid volume flow rate, the laminar ( $d_i = 1.95$  mm) and the turbulent ( $d_i = 1.3$  mm) liquid flow regime show drastically different distributions of mass flux density. In contrast for the laminar case at a distance of 25 mm downstream the nozzle, a distinct peak of the mass flux density exists at the spray axis, for the turbulent jet the mass flux density is about half an order of magnitude smaller. These differences are confirmed by light sheet photographs taken at the nozzle exit. Even 200 mm downstream a distinct maximum of the mass flux density is apparent for the laminar liquid jet. It should be mentioned that this great change in spray characteristics also leads to an increase in the total entrainment rate of the expanding two phase flow of about 50 % when exceeding the laminar–turbulent transition. This is extremely important for all processes for which rapid mixing of the surrounding gas with the two phase flow is desired.

In order to investigate the influence of liquid viscosity, this was varied by varying the temperature of the liquid and by using different liquids. In Fig. 6 the pressure drop at the air side is shown for four viscosities at different temperatures of the same liquid. As in Fig. 3 there is a strong increase of the pressure drop at about  $Re = 3000$ . Along the laminar regime, the pressure drop at constant Reynolds number is equal for all viscosities although the liquid volume flow rate is different. In this region, the pressure drop is mainly governed by the annular air flow in the nozzle exit. In the turbulent regime, the pressure drop for constant Reynolds number strongly depends on the liquid volume flow rate because the nozzle exit is filled with a two-phase flow. For two-phase flow, the sonic velocity decreases with increasing liquid volume fraction and, hence, with the liquid volume flow rate. Since the gas flow is kept

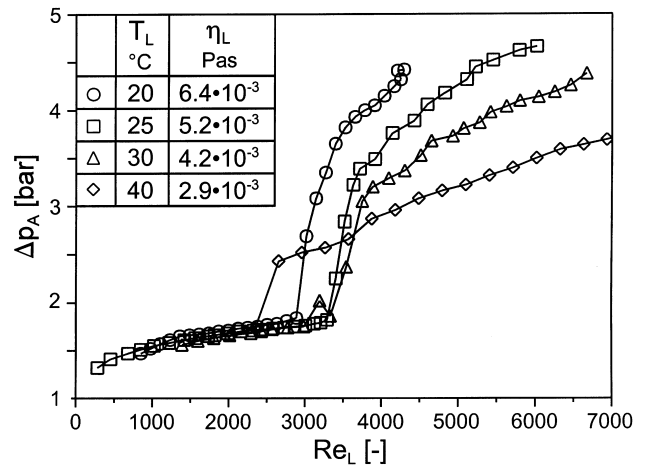


Fig. 6. Air pressure drop  $\Delta p_A$  as a function of Reynolds number for different viscosities of the liquid phase,  $\dot{V}_A = 5.9 \text{ m}^3/\text{h}$ ,  $d_o = 2.4 \text{ mm}$ ,  $d_i = 1.3 \text{ mm}$ ,  $l_o = 2 \text{ mm}$ ,  $l_i/d_i = 20$ .

constant, the gas density and the pressure drop must increase for decreasing sonic velocity. For the spatial distribution of the  $D_{32}$  a similar behavior to that with the variation of the inlet-port diameter could be observed. For all laminar cases, the maximum of the  $D_{32}$  could be detected at the spray axis, independent of the individual liquid viscosity, whereas for turbulent cases an even profile with a similar average  $D_{32}$  has been achieved.

For technical applications the inlet duct is usually shorter than the length required for fully developed flow; the required length for laminar flow is  $130 d_i$  and for turbulent flow  $50 d_i$ . The appearance of transition from laminar to turbulent flow depends on the state of development of the flow. Fig. 7 shows the pressure drop of the air for three different length-to-diameter ratios ( $l_i/d_i$ ) of the inlet port. The ratio  $l_i/d_i = 20$  shows the most stable laminar flow (late transition). The transition is restricted to a small region at about  $Re = 3000$ . For smaller ratios of  $l_i/d_i$  the distortion of the liquid surface

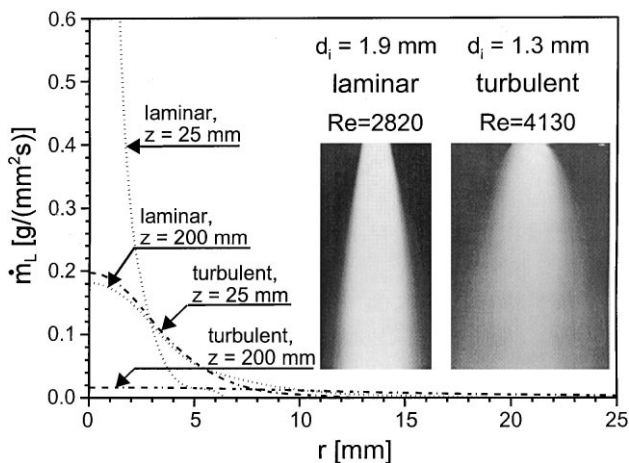


Fig. 5. Radial profiles of mass flux density  $m_L$  for laminar and turbulent liquid flow regime,  $\dot{V}_L = 70 \text{ L/h}$ ,  $\dot{V}_A = 5.9 \text{ m}^3/\text{h}$ ,  $d_o = 2.4 \text{ mm}$ ,  $l_o = 2 \text{ mm}$ ,  $l_i/d_i = 10$ .

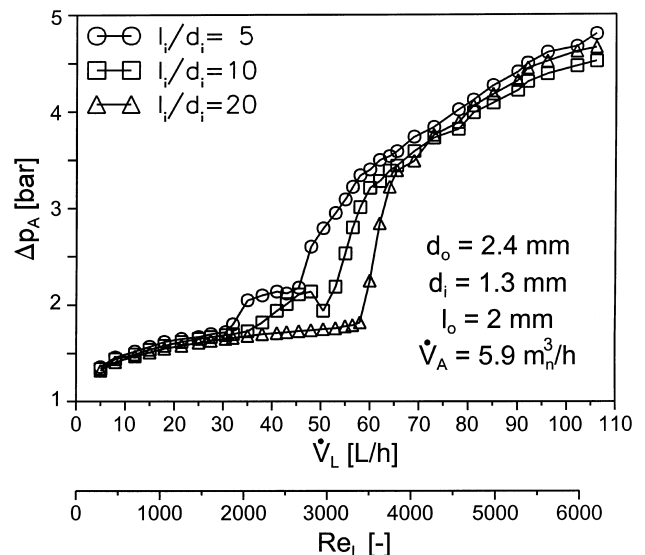


Fig. 7. Air pressure drop  $\Delta p_A$  as a function of liquid volume flow rate for different ratios of length to diameter ( $l_i/d_i$ ) for the liquid inlet.

starts earlier and a transition region with fluctuations in pressure occurs. Fig. 8 shows  $D_{32}$  distributions corresponding to  $Re = 3250$ . The ratio of  $l_i/d_i = 20$  still shows a laminar profile, whereas the shorter ratios of  $l_i/d_i$  show a nearly even profile which is characteristic for turbulent liquid flow. The differences in the average  $D_{32}$  between  $l_i/d_i = 5$  and  $l_i/d_i = 10$  may be explained by different exit conditions, i.e. the degree of turbulence of the liquid jet when leaving the inlet port.

3.3. Governing parameters for transition to cavitation

Cavitation is caused by an increase in the dynamic pressure at the flow restriction inside the inlet port (see Fig. 1). As a consequence, the static pressure reaches the magnitude of the vapor pressure. The vapor bubbles formed collapse after a short time downstream of the inlet port, generating additional disturbances on the liquid jet surface and tearing droplets from the jet surface. These droplets can be seen as cone-shaped deposits on the window (Fig. 2-VI). In contrast to the non-cavitating jet (IV) the first visible part of the liquid jet is opaque due to dispersed vapor bubbles. According to Fig. 9, the improvement of atomization quality due to the onset of cavitation is negligible, and a slight deterioration of the droplet diameter symmetry may be observed. The mean velocity of the droplets is also nearly unaffected by transition to cavitation (Fig. 9). Further increase in liquid volume flow rate is followed by increased cavitation. As a result, a flow structure similar to Fig. 2 VII appears with drastic asymmetry of the spray. It is worth mentioning that, at this flow condition, a slight increase in the air mass flow rate, coupled with an increase in pressure inside the mixing chamber, could reconvert this state of flow to the stable cavitating flow condition marked in Fig. 2 with VI.

3.4. Influences other than liquid flow characteristics

According to Fig. 10, with increase of the gas flow rate the transition region moves slightly to smaller Reynolds numbers, which can be attributed to stronger aerodynamic forces. However, the general appearance of the  $D_{32}$  profiles remains the same. For all air flow rates with a laminar liquid flow, a distinct peak was observed at the spray axis, whereas for the turbulent liquid jet an nearly even profile has been obtained. However, as expected, the  $D_{32}$  decreases for both flow conditions over the entire cross section with increasing gas flow rate.

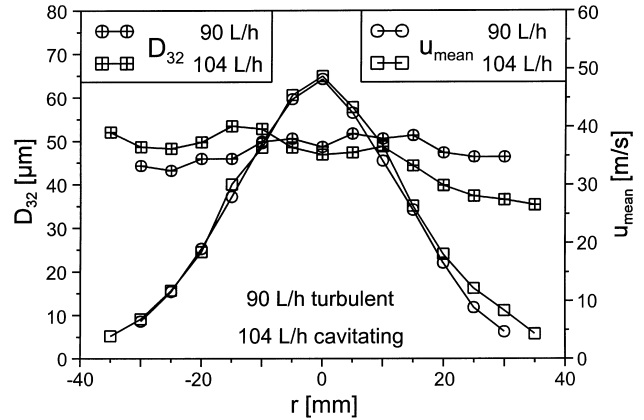


Fig. 9. Radial profiles of local  $D_{32}$  and  $u_{mean}$  for turbulent and cavitating liquid flow,  $\dot{V}_A = 5.9 \text{ m}^3/\text{h}$ ,  $d_o = 2.4 \text{ mm}$ ,  $l_o = 2 \text{ mm}$ ,  $l_i/d_i = 10$ .

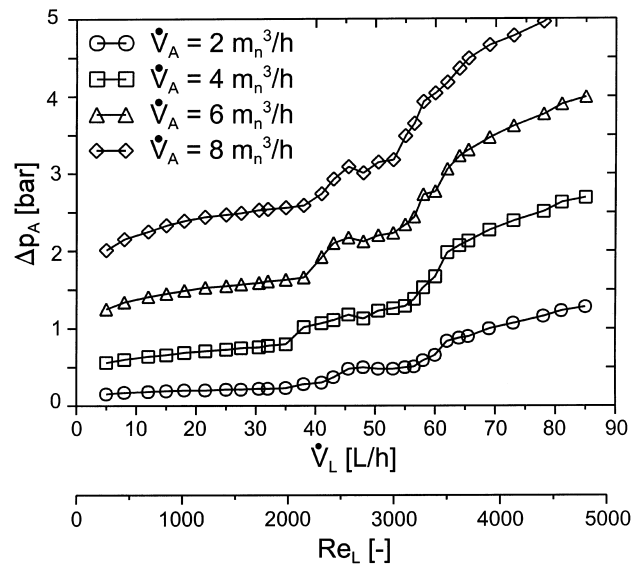


Fig. 10. Air pressure drop  $\Delta p_A$  as a function of the liquid flow rate or liquid flow Reynolds number,  $d_o = 2.4 \text{ mm}$ ,  $l_o = 2 \text{ mm}$ ,  $l_i/d_i = 10$ .

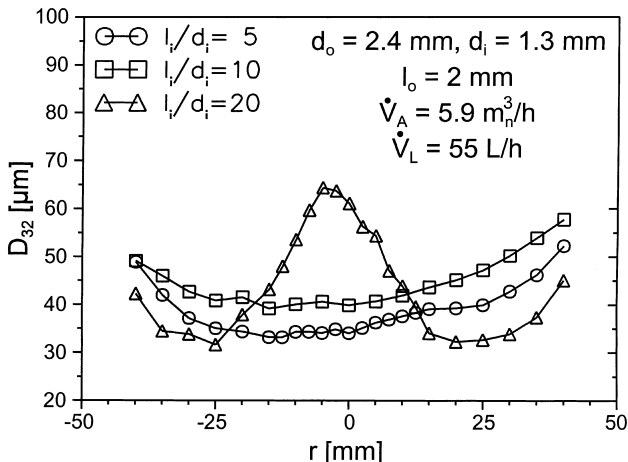


Fig. 8. Radial profiles of local  $D_{32}$  for different length to diameter ratios ( $l_i/d_i$ ) for the liquid inlet.

In addition, the length to diameter ratio ( $l_o/d_o$ ) of the outlet port has a strong influence on the spray characteristics (Kufferath et al., 1996). For high ratios of  $l_o/d_o$  ( $\geq 4$ ) the influence of the inlet characteristics of the liquid jet disappears. Now, for laminar liquid flow also an even  $D_{32}$ -profile has been obtained, because the residence time of the two-phase flow in the outlet port is sufficiently long for a nearly complete liquid-phase disintegration, and therefore one ends up with the two phase flow covering the whole cross-section of the outlet port. In this case, the profiles for the laminar and turbulent cases are nearly the same. Nevertheless, it must be considered that the length of the outlet port has a strong influence on the spray characteristics (Kufferath et al., 1996). The distance between the inlet port for the liquid and the beginning of the outlet port of the nozzle (mixing chamber length) is of minor importance within the investigated range from 5 to 15 mm. However, for a mixing chamber length shorter than 5 mm in the turbulent and the laminar case, the time is too short for sufficient distortion of the liquid jet. Therefore a slight increase of the  $D_{32}$  diameter distribution was observed over the entire cross-section.

#### 4. Conclusions

The flow characteristics of a liquid jet leaving the inlet port have a strong influence on the radial distributions of the  $D_{32}$  droplet diameter and the mass flux density in the spray. For short outlet ports ( $l_o/d_o \lesssim 2$ ), the maximal  $D_{32}$  mean droplet diameter for laminar liquid jet is found on the spray axis, whereas turbulent liquid jets lead to a nearly even radial profile. The turbulent liquid jet leads to a much broader distribution of the dispersed liquid phase downstream of the nozzle. For long outlet ports ( $l_o/d_o \gtrsim 4$ ), however, even profiles are found in either case.

Transition between both regimes of spray characteristics turned out to be really a function only of the liquid flow Reynolds number. The transition region should be avoided in technical applications due to an unsteady behavior of the spray. Furthermore, the volume flow rate for the liquid should be limited below the onset of cavitation, because its effect on the disintegration mechanism cannot be well predicted and may lead to spray jet asymmetries.

#### References

- Chigier, N.A., 1991. The Physics of Atomization, In: Proc. ICLASS-91, Gaithersburg, MD, USA., pub NIST 813, pp. 1–15.
- Faragó, Z., Chigier, N.A., 1992. Morphological classification of disintegration of round liquid jets in a coaxial air stream. *Atomization and Spray Tech.* 2, 137–153.
- Gelfand, B.E., 1996. Droplet breakup phenomena in flows with velocity lag. *Progress Energy Combustion Science* 22, 201–265.
- Kufferath, A., Heyse, C., Leuckel, W., 1996. Influence of outlet port length on liquid atomization by an air-assisted internal-mixing nozzle. In: Proc. ICLASS 96, Lund, Sweden, pp. 179–184.
- Kufferath, A., Leuckel, W., 1997. Experimental investigation of flow conditions inside an air-assisted internal-mixing nozzle and their correlation with spray data. In: Proc. ICLASS 97, Seoul, South Korea, pp. 262–269.
- Lefebvre, H., 1989. Properties of Sprays. *Particle and Particle Systems Characterization* 6, 176–186.
- Lorenzetto, G.E., Lefebvre, A., 1977. Measurements of drop size on a plain-jet airblast atomizer. *AIAA Journal* 15 (7), 1006–1010.
- Mansour, A., Chigier, N., 1994. Effect of turbulence on the stability of liquid jets and the resulting droplet size distribution. *Atomization and Sprays* 4, 583–604.
- Nukiyama, S., Tanasawa, Y., 1938. An experiment on the atomization of liquid by means of an air stream. *Trans. Soc. Mech. Engrs. (Japan)* 4/5, 13–17.
- Ohrn, T.R., Senser, D.W., Lefebvre, A.H., 1991. Geometric effects on discharge coefficients for plain-orifice atomizers. *Atomization and Sprays* 1, 137–153.
- Ramamurthi, K., Nandakumar, K., 1994. Disintegration of liquid jets from sharp-edged nozzles. *Atomization and Sprays* 4, 551–564.
- Sato, K., Okiura, K., Shoji, K., Akiyama, I., Takahashi, Y., 1988. Experimental study on the atomization process of slurry fuels. In: Proc. ICLASS 88, Sedai, Japan, pp. 73–80.
- Schweitzer, P.H., 1937. Mechanism of disintegration of liquid jets. *J. Appl. Phys.* 8, 513–521.
- Shavit, U., Chigier, N., 1994. Turbulence flow characteristics in a special atomizer. In: Proc. ICLASS 94, Rouen, France pp. 205–212.
- Wu, P.K., Faeth, G.M., 1993. Aerodynamic effects on primary breakup of turbulent liquids. *Atomization and Sprays* 3, 265–289.
- Wu, P.K., Miranda, R.F., Faeth, G.M., 1995. Effect of initial flow conditions on primary breakup of nonturbulent and turbulent round liquid jets. *Atomization and Sprays* 5, 175–196.
- Yule, A.J., Dalli, A.M., Yeong, K.B., 1998. Transient cavitation and separation in a scaled-up model of a VCO orifice. In: Proc. ICLASS 98, Manchester, UK, pp. 230–235.